Conf-920631--17

WSRC-MS--91-269

DE92 010633

ACCEPTANCE CRITERIA FOR HEAT EXCHANGER HEAD STAYBOLTS (U)

by

R. L. Sindelar, P. S. Lam, D. M. Barnes, A. Placr, and J. M. Morrison

Westinghouse Savannah River Co.
Savannah River Site
Aiken, South Carolina

A paper proposed for presentation at the
1992 ASME PUP Conference
New Orleans, Louisiana
June 21 - 25, 1992

and for publication in the proceedings

This paper was prepared in connection with work done under Contract No. DE-AC09-89SR18035 with the U.S. Department of Energy.

"Acceptance Criteria for Heat Exchanger Head Staybolts" (U)

by

P.S. Lam, R. L. Sindelar, D. M. Barnes, Arnost Placr, and J. M. Morrison
Westinghouse Savannah River Company
Aiken, SC 29808

ABSTRACT

Each of the six primary coolant loop systems of the Savannah River Site production reactors contains two parallel single-pass heat exchangers to transfer heat from the primary coolant (D_2O) to the secondary cooling water (H_2O). The configuration of the heat exchangers includes a plenary space defined by the heat exchanger tubesheet and the heat exchanger head at both the heat exchanger inlet and outlet to the primary piping. The primary restraint of the heat exchanger head (Type 304 stainless steel) is provided by 84 staybolts (Type 303 stainless steel) which attach to the tubesheet. The staybolts were cap seal-welded in the mid-1960's and are immersed in moderator. Access to inspect the staybolts is limited to a recently-developed ultrasonic technique shooting a beam through the staybolt assembly.

Acceptance Criteria to allow disposition of flaws detected by UT inspection have been developed. The structural adequacy to protect against collapse loading (ASME BPVC Section III, Appendix F) of the head is demonstrated by finite element analysis of the head assembly and fracture analysis of flaw postulates in the staybolts. Both normal operation and normal operation plus seismic loading conditions were considered. Several bounding cases containing various configurations of nonactive (exceeding critical flaw size) staybolts were analyzed. The model of the head assembly can be applied to evaluate any active staybolt configurations based on the results from future inspections.

INTRODUCTION

The demonstration of structural integrity of the primary coolant piping system of the Savannah River Site (SRS) production reactors includes evaluating the structural capacity of each component against a large break or equivalent Double-Ended Guillotine Break. There are twelve heat exchangers, two connected in parallel flow in each of six primary coolant loops, which provide once-through cooling of the D_2O moderator/coolant. A large break at the inlet and outlet heads of the heat exchangers would occur if the restraint members of the heads would become inactive. The SRS heat exchanger head is a funnel-shaped structure attached to the tubesheet by 84 staybolts (see Figure 1). The other end of the head is attached to the PWS piping at the pipe flange. In addition to the staybolts, the head is also supported by secondary load carrying components such as the c-clamps and the half-pipe seals across the head flange and the tubesheet flange. These components are primarily used for leakage prevention. Access to the staybolts is limited due to a welded seal cap over the staybolts. An UT inspection technique to provide an in-situ examination of the staybolts has recenctly been developed at SRS.

This report provides an Acceptance Criteria methodology with the technical bases to: disposition flaws reported in the staybolt inspections; ensure adequate restraint capacity of the staybolts maintaining allowable safety margins; and provide an approach for the baseline and periodic inspections of the staybolts ensuring that any degradation to the staybolts reducing their load carrying capacity would be detected and monitored.

The adequacy of head restraint, even with flawed staybolts, is demonstrated by performing stress analysis of the heat exchanger head and staybolts and a fracture mechanics analysis of the staybolt flaws. A three dimensional finite element model was developed for the head and staybolts. Normal operating pressure and piping seismic reactions forces were applied to the model. The critical flaw depths for individual staybolts and various configurations of multiple inactive staybolts were estimated by linear elastic fracture mechanics. Acceptance Standards for flaw disposition were developed by applying a safety factor of three on the staybolt stresses to calculate instability lengths for postulated flaws. The finite element program for stress analysis was developed to support any future UT inspections of the staybolts and would allow evaluation of various customized, inactive staybolt configurations based on the inspection results.

The purpose of the present work is to develop acceptance criteria for staybolts should flaws be detected in the UT inspection. The load carrying capacity of the secondary components (c-clamps and half-pipe seals) is ignored in the analysis of staybolt loading and the calculation of flaw instability depths.

SRS HEAT EXCHANGERS

The heat exchangers are horizontal, saddle-mounted cylindrical tanks (bounded by shell and tubesheets) about 33.5 feet long and 7.5 feet in diameter. The moderator enters the heat exchanger head-tubesheet plenum space and is distributed to about 9000, 1/2" OD and 0.049" nominal thickness tubes through the river water secondary coolant and exits from the outlet end. The head is attached to the tubesheet by 84 staybolts, each of them has a 1960's redesign of inverted pipe cap seal welded to the top of the bushing, as a pressure seal. A half pipe ring was welded to the flanges of the head and tubesheet to prevent leakage. This attachment is also supported by 72 forged c-clamps in the flange areas as secondary load carrying components. The heat exchangers are mounted on two rail trucks with seismic bracing to anchor them firmly to the floor. The configuration can be seen in Figure 1.

Materials of Construction and Service Conditions

The present arrangement of heat exchangers in K and L reactors contains head and shell material of either Type 304 or 304L stainless steel and staybolt material of Type 303 stainless steel. When new heat exchangers were procured, modifications were made to the design to eliminate problems that were encountered with the original Foster Wheeler heat exchangers. Significant changes were made to the design of the heat exchangers procured from Mitsui and Hitachi in 1983. The leak collection spaces were eliminated, the tube and tube sheets were made of 316L, and the shell nozzles, distributor plates, baffle spaces and heads were made of 304L SS. These parts in the original heat exchangers were made of 304 SS. All of the modifications made to the Mitsui and Hitachi heat exchangers were also incorporated in the Nooter heat exchangers. In addition, Sea Cure tubes (ferritic SS) were used in the Nooter design rather than 316L SS. All twelve heat exchangers in L Area are Mitsui with new heat exchanger heads of 304L SS, all 12 in P Area are Foster Wheeler, and K Area has 1 Nooter, 1 Mitsui, and 10 Foster Wheeler units. Tensile properties (yield,

tensile, and flow strengths and Young's modulus) are provided for each of Types 304, 304L, and 303 stainless steel.

The heat exchanger operating and design conditions are summarized in Table 1:

TABLE 1. Heat Exchanger Operating and Design Conditions

		PW Inlet	PW Outlet	CW Inlet	CW Outlet
Temperature (°F)	Operating	203	104	68	194
	Design	250	250	200	200
Pressure (psig)	Operating	218†	163†	50	20
	Design	300	300	150	150

Mechanical Properties for Engineering Analysis

The heat exchanger staybolt material is Type 303 stainless steel. The tensile strength and yield strength of Type 303 stainless steel at room temperature, 100°F, and 200°F is shown below:

TABLE 2. Tensile Strength and Yield Strength for Type 303 SS

Material	Temperature (°F)	Tensile Strength (ksi)	Yield Strength (ksi)
Type 303 SS	70	75	30
	100	74†	30†
	200	71†	30†

(References 1 and 2)
† Linear interpolation from other Reference 2 values

Type 303 SS mechanical properties are similar to Type 304 SS at room temperature as shown in Tables 2 and 4. The ASME B31.1 & B31.3 construction codes and the ASME BPV code do not specify fracture toughness properties for austenitic stainless steels. Therefore, the fracture toughness data shown in Table 3, obtained from the RMP baseline testing for Type 304 SS at 257 °F, is the recommended fracture toughness parameter for Type 304 SS and Type 304L SS. No significant difference in toughness between Type 304 SS and Type 303 SS is expected since the compositions and product forms are similar. Therefore, the properties in Table 3 are recommended for the fracture toughness of the Type 303 SS staybolt material:

TABLE 3. Fracture Toughness for Types 304, 304L and 303 SS

Material	Test Temperature (°F)	Sample ASTM Orientation	J_{Ic}-Deformation (kJ/m^2)	K_{Ic}-Deformation ($Mpa\sqrt{m}$)
304 ss Base	257	C-L	338	258

(Reference 3, Table 5-4).

The heat exchanger head and shell material is either 304 SS or 304L SS depending on the heat exchanger manufacturer. Since the computer model of the heat exchanger head assembly is being developed to support any future UT inspections of the staybolts, the mechanical properties for 304L SS were used in the analysis as the tensile strength of Type

304L SS is bounding. Mechanical properties for Type 304 SS and Type 304L SS at various temperatures are provided in Table 4:

TABLE 4. Material Properties for Type 304 and 304L SS

Material	Temp. (°F)	Design Stress Intensity S_m (ksi)	Yield Strength S_y (ksi)	Tensile Strength S_u (ksi)	Young's Modulus E (psi)	Flow Stress (ksi) ††
Type 304	70	20†	30	75	28.3×10^6	60
	100	20	30	75	28.1×10^6†	60
	200	20	25	71	27.6×10^6	60
Type 304L	70	16.7†	25	70	28.3×10^6	50.1
	100	16.7	25	70	28.1×10^6†	50.1
	200	16.7	21.3	66.2	27.6×10^6	50.1

(Reference 2 and Reference 4, Table I-1.2, Table I-2.2, Table I-6.0 and Table I-3.2)
† Linear interpolation from other Table 4 values
†† The flow stress is given as 3 S_m as suggested in Reference 5.

In the finite element analysis, Young's Modulus is identical for these two stainless steels, 27.6×10^6 psi. Both materials are assumed to behave with elastic-perfectly plastic response (nonhardening) with effective yield stresses taken to be three times the ASME stress intensities, S_m. This is consistent withthe General Electric piping analysis scheme (Ref.5). The effective yield stresses are thus 50.1 ksi for the head, and 60 ksi for the staybolts. Poisson's ratios are 0.3 for both stainless steels.

For the collapse load analysis of a head with inactive staybolts, the effective yield stresses for the head and the staybolts were 2.3 times S_m , i.e., 38.41 ksi and 46.0 ksi, respectively. The multiplier of 2.3 is given in the ASME Boiler and Pressure Vessel Code Section III, Division 1, Appendix F, Article F-1341.3 for limit load analysis.

HEAT EXCHANGER SERVICE HISTORY SUMMARY

The reactor process water heat exchangers have operated successfully without gross rupture or failure of the heads (primary pressure boundary), tubes (primary to secondary pressure boundary), or shells (secondary pressure boundary) throughout service. During the past 36 years of reactor operation, representing over 400 heat exchanger years of operation, approximately 60 instances of leakage have occurred through the pressure boundaries which were remedied by repair of, replacement of, or design modifications to the heat exchangers. Many heat exchangers were repaired or replaced because of tube leaks. Most of the tube cracking resulting in leakage of moderator into the secondary coolant was due to vibration fatigue or corrosion. Corrosion mechanisms have also caused cracking in other parts of the heat exchangers including the head, staybolts, and shell. Additional heat exchangers were procured through the years with design improvements to reduce or eliminate these degradation mechanisms. The newest design by Nooter Corporation incorporates design features that should eliminate all of the significant degradation mechanisms leading to leakage. Crevice corrosion of the head staybolts is the only remaining postulated degradation mechanism in the Nooter design, the most recent of the heat exchanger designs in service.

FINITE ELEMENT ANALYSIS OF HEAT EXCHANGER HEAD

A finite element model of the heat exchanger head is constructed for analyzing the loads acting on the staybolts due to the process water pressure and piping reaction forces from seismic loadings. The three-dimensional model can accommodate the asymmetric geometry if some of the staybolts become inactive due to flaw depths exceeding calculated instability lengths. Staybolt loads will be used as input to the linear elastic fracture mechanics analysis for flaw instability. the staybolt flaw disposition is based on flaw instability depths calculated for various configurations of inactive staybolts.

Finite Element Model

The head of heat exchanger itself is an axisymmetric structure and the staybolt arrangement is octagonally symmetric. However, in the development of acceptance criteria some of the staybolts are deactivated due to postulated flaws exceeding calculated instability depths. Therefore, this limited symmetry is destroyed and a full three-dimensional finite element model must be considered. To reduce the model size, three-dimensional shell elements were adopted to model the head. Large rotations were expected to occur in the cases of several staybolt failures in a grouped arrangement. The nonlinear geometry option, NLGEOM, was therefore specified.

The model was generated with PATRAN (Ref.6) finite element pre/post-processor according to engineering drawings for the shape of the head and the locations of 84 staybolts and 72 c-clamps. The PATRAN model was transformed to a finite element mesh for the ABAQUS code (Ref.7) on SRS Cray X-MP EA Supercomputer.

The finite element mesh (Fig.2) contains 1008 thin shell elements (S4R5) for the majority of the heat exchanger head, 216 thick shell elements (S4R) for the pipe flange and the head flange, and 300 beam elements (B31, including 84 dummy elements representing the bosses above the head to identify the staybolt locations) for 84 staybolts which have 5 different lengths. The finite element mesh design for the heat exchanger head must accommodate the exact locations of the 84 staybolts.

Two to seven beam elements were used to represent the partial length of a staybolt between the head and the tubesheet. The shortest staybolt is 8.875". However, the shortest distance between the centerline of the head and the tubesheet is approximately 2.5". Based on the load transfer mechanism of the staybolt assembly, the distances between the head and tubesheet were considered to be the effective lengths of the staybolts .

A total of 1596 nodes were used for the model. An additional node was used for tying together all individual degrees of freedom of the pipe flange nodes by the Multi-Points Constraints (MPC) option in ABAQUS. This insures that the nodes connected to the piping system will deform in the same manner. This additional node and MPC were not used in the Teledyne case.

A thickness of 1.5" was input as the averaged head thickness in the finite element model. The thicknesses for the pipe flange and the head flange were estimated to be 4.5" and 2.875", respectively. The nominal shaft diameter of the staybolts is 2", however, the narrowest diameter of the staybolts is 1.567" near the threaded ends and was used in the model.

The PWS pressure is maintained at 230 psi in the head plenum space, even when some staybolts are inactive resulting in a separation of the head flange from the tubesheet flange. This pressure bounded the normal operating pressure reported earlier. The tubesheet was not modelled in this analysis and the tubesheet ends of the staybolts were fixed in space at their original locations.

A set of piping seismic reaction forces, calculated by URS/John A. Blume & Associates, Engineers (Ref.8), was applied to an extra node to which all pipe flange nodes were tied by MPC. This treatment forces those nodes to deform coincidently because the pipe flange is physically bolted to the PWS piping system. The piping reaction forces had insignificant impact on the cases examined. For example, the maximum reaction force in the axial direction of the heat exchanger was 4,137 lbs (Ref.8, page 6-10, System 2 - Area 105-C, Node 32, Design Load = Gravity ± Seismic). On the other hand, the axial reaction force due to 230 psi pressure loading alone was 1.54 million lbs from the finite element results. As long as the majority of the staybolts are intact, the piping reaction forces are insignificant. Similar observations are obtained for the piping moments calculated by the same source. The piping reaction forces applied to this model for all calculations (except the Teledyne case) correspond to the Design Loads of System 1 - Area 105-C, in Blume Report (Ref.8) page 6-5, Node 31: The axial force was 3,106 lbs; lateral forces were 624 and 1,192 lbs; axial moment was 43,143 in-lb; and the lateral moments were 106,393 and 40,209 in-lb.

Staybolt Loading Analysis

The forces acting on the staybolts due to the PWS pressure (primary loading) and piping reaction forces (insignificant except at large numbers of inactive staybolts) were calculated as input to the fracture analysis to determine staybolt flaw instability lengths. The axial tension (the tensile force along the staybolt axis) was the dominant force component in the cases considered (i.e., majority of the staybolts were still active). Therefore, the bending effects can be neglected in the fracture analysis. The axial force was used as a criterion for the subsequent removal of staybolts resulting in worst configurations of inactive staybolts, and was used in the fracture mechanics evaluation of the instability flaw depth (a_{cr})

Figure 3 is the staybolt arrangement map. The numbers inside the parentheses are the finite element node numbers from which the staybolt reactions can be read off in the ABAQUS output. These reactions are in fact the staybolt loads with their signs changed (or the directions of the forces reversed). Note that Figure 3 is the staybolt arrangement viewing from the tubesheet, i.e., the axial direction of the heat exchanger head is +Y-direction (see Figure 2 for the coordinate system, and in Figure 3 the +Y-direction is perpendicular to the paper and pointing downward). The algorithm of removing highest stressed staybolts for the intact head and for the subsequent configurations is as followed:

1. Load 230 psi water pressure and piping reaction forces (Ref.8) to the heat exchanger head with all 84 staybolts active. Without the piping reaction forces, the highest stressed staybolts occur equally at 12 remote corners of the staybolt arrangement map (see Figure 3, Staybolt Numbers A01, A04, A05, A38, A56, A74, A84, A81, A80, A47, A29 and A11). It was discovered that the load transfer is the most severe when these corner staybolts become inactive. The perturbation due to the piping reaction forces was minor, but gave a preferential failure direction initiating at one of the corner staybolts. For a particular set of piping reaction forces used in the analysis, staybolt A29 was the highest stressed.

2. After the calculation of Step 1 is complete, the maximum staybolt axial tension, $(P_{max})_o$ (denoted by RF2 in the ABAQUS output for nodal reactions in the Y-direction), and the node number are found. The corresponding staybolt number can be located by using Figure 3 as a guide. In the present case, it was 35,300 lbs at staybolt A29. This axial tensile force is used to calculate $(a_{cr})_o$, the critical flaw size or instability length for the case of zero inactive staybolts.

3. Staybolt A29 is removed from the model and the applied loads (pressure and piping reaction forces) remain unchanged. Recalculate the staybolt loads.

4. Find the maximum staybolt tensile load, $(P_{max})_i$ for the configuration of Step 3. The corresponding critical flaw size, $(a_{cr})_i$, is calculated by fracture analysis.

5. Remove all staybolts with axial tensile forces exceeding $(P_{max})_o$, the maximum tensile force acting on the staybolts in the intact head configuration (obtained in Step 2).

6. With the new configuration, recalculate the staybolt loads with the applied loads fixed.

7. Repeat steps 4 to 6, until a_{cr} is below UT resolution or the number of the inactive staybolts becomes unacceptable according to the collapse load analysis.

STAYBOLT FRACTURE ANALYSIS

The forces experienced by the staybolts calculated in the finite element analysis can be used to estimate the critical flaw length (or depth, with respect to the staybolt diameter). The axial tension was the dominant force component in our case. This force component was used as the remote tension acting on a flawed sample (Fig.4). In the center of the three-dimensional crack front, plane strain condition prevails. Based on these assumptions, the fracture instability criterion was calculated with linear elastic fracture mechanics. The stress intensity factor, K_I , for a plane strain finite plate under remote tension (Fig.3) is given in Reference 9:

$$K_I = \sigma\sqrt{\pi a}\ F\left(\frac{a}{b}\right) ,$$

where

$$F\left(\frac{a}{b}\right) = \sqrt{\frac{2b}{\pi a}\tan\frac{\pi a}{2b}}\ \frac{0.752 + 2.02\frac{a}{b} + 0.37\left(1 - \sin\frac{\pi a}{2b}\right)^3}{\cos\frac{\pi a}{2b}}$$

and

$$\sigma = \frac{4}{\pi D^2} \times (\text{Axial Tension Load}) .$$

In the above expressions, a is the length (depth) of the flaw, b is the width of the plane strain plate or the diameter (D = 1.567") of the staybolt. The flaw is assumed to reach its critical or instability length ($a = a_{cr}$) when $K_I = K_{IC}$, where K_I is the stress intensity factor due to the applied tensile stress σ and K_{IC} is the fracture toughness of the material. The fracture toughness for staybolt material, 303 Stainless Steel, is selected from the Reactor Materials Program baseline testing of archive Type 304 Stainless Steel. The fracture toughness for this calculation was 258 Mpa$\sqrt{m}$, or 235 ksi$\sqrt{in}$.

For this given fracture toughness and the finite element calculated axial tensile forces on the staybolts, the critical flaw lengths can be obtained by solving the above set of nonlinear equations. The result is shown in Table 5 and plotted in Figure 5.

TABLE 5 Instability Flaw Lengths (Depths) for Various Staybolt Configurations (Staybolt Diameter = 1.567 inches)

No. of Inactive Staybolts	Instability Flaw Length (% of Staybolt Diameter) Based on Actual Forces	Instability Flaw Length (% of Staybolt Diameter) Safety Factor = 3
0	71.3	49.2
1	66.1	41.7
3	59.3	32.7
6	51.3	23.5
10	47.2	19.2
17	46.4	18.5

Table 5 includes the critical flaw sizes with a Safety Factor of 3 (SF=3) applied to the calculated staybolt axial forces. These data points are labelled on the curve in Figure 5.

COLLAPSE LOAD ANALYSIS

The collapse loads for heat exchanger head with various inactive staybolt configurations were analyzed according to ASME Boiler and Pressure Vessel Code Section III, Division 1, Appendix F, Article F-1341.3. The calculated load-deflection curves, plotted as the pipe flange axial displacement versus the water pressure, are shown in Figure 6 for an intact head and a head with 10 inactive staybolts.

As mentioned earlier, the ASME Code requires that the equivalent yield stresses for the materials be reduced to 2.3 S_m. The same piping reaction forces were applied to the pipe flange as in Section 3.3.3. The numerical procedure was stable when the pressure was increased to 690 psi (3 times the operating pressure) for an intact head. For a head with 10 inactive staybolts, the ABAQUS program had a convergence problem at 305 psi. However, by applying ASME II-1430 and reference figure II-1430-1 to the load deflection curve for 10 inactive staybolts (Fig.6), the collapse load would be beyond the bounding normal operating pressure, 230 psi. Therefore, even with 10 inactive staybolts, the head is still considered to be structurally acceptable. On the other hand, for the case of 17 inactive styaybolts, the collapse load is below the normal operating pressure. Therefore, it is concluded that the case of 10 inactive staybolts would be the limiting configuration for the heat exchanger head.

HEAT EXCHANGER STAYBOLT ACCEPTANCE CRITERIA

An Acceptance Criteria Methodology is produced for the disposition of UT inspections results of the heat exchanger staybolts should flaws be detected. The methodology is shown schematically in Figure 7. Acceptance Standards are developed for various configurations of inactive staybolt distributions using the instability flaw depths calculated by linear elastic fracture mechanics.

A three-dimensional finite element analysis was carried out to calculate the forces acting on the staybolts under the bounding normal operating pressure 230 psi and a set of piping reaction forces. The piping reaction forces were applied to maintain the PWS piping-heat exchanger structural assembly, and it was shown that their magnitudes were insignificant compared to the total reactions due to the operating pressure alone. In the finite element model the heat exchanger head material is 304L stainless steel, and the staybolt material is 303 stainless steel.

Various inactive staybolt configurations were analyzed. The highest stressed staybolts were the shortest length located at the corners of octagonal sectors of the overall staybolt arrangement on the head. It was found that and the maximum load transfer occurred when a corner staybolt was inactive. For inactive staybolts located at different sectors, the load transfer was usually insignificant. Based on these observations, various inactive staybolt configurations were sequentially analyzed by progressively deactivating neighboring staybolts. During the calculations the normal operating pressure was maintained for all configurations. The results of these bounding cases were used to develop the staybolt acceptance criteria.

The axial force in tension dominated the failure process of the flawed staybolts. The calculated axial forces acting on the staybolts were used to estimate the critical (or instability) flaw depth (with respect to the diameter of staybolts) based on a linear elastic fracture mechanics solution for a plane strain edge crack in a finite specimen. A safety factor of 3 (SF=3) was applied to the staybolt axial forces calculated under the normal operating conditions plus the piping reaction forces under a seismic event (or the Design Load in Ref.8).

Acceptance Criteria Methodology - Inactive Staybolt Combinations

The heat exchanger staybolt Acceptance Criteria Methodology is presented schematically in Figure 7. The acceptability of flawed staybolt configurations is based upon Acceptance Standards for flawed staybolts for cases from zero to 10 grouped inactive staybolts. Guidance for combining flawed staybolts to determine grouping number (zero to 10) for inactive staybolts is given below. The results of finite element stress analysis and linear elastic fracture mechanics are summarized here to develop the acceptance criteria. Note that the safety factor of 3 is applied to the staybolt loads.

1. If flawed staybolts are found in the opposite sides of the heat exchanger head, the individual criterion may be applied, i.e., flaw depth is 49.2% of the diameter (1.567") in the narrowest part of the staybolt (see Table 5).

2. If multiple staybolts are found in a close vicinity, the adjacent inactive staybolts criterion may be applied according to Table 5.

3. Based on a conservative ASME collapse load analysis, the total number of inactive staybolts may not exceed 10. Note that a flawed staybolt is considered to be inactive if either or both of the previous criteria are met.

Acceptance Standards for Flawed Staybolts

The ultrasonic test inservice inspection may report a list of flawed staybolts with various flaw depths. To determine how many of these staybolts are classified as inactive and whether flawed staybolt configuration is allowed for continued service without replacing flawed staybolts, Table 7 is established for the staybolt flaw acceptance criteria:

TABLE 7 Acceptance Criteria for Critical Flaw Depths
(The staybolt loadings are 3 times normal operating plus piping reaction forces including seismic forces applied to the heat exchanger head)

Configurations: No. of Inactive Staybolts (i)	Critical Flaw Depths ($a_{cr,i}$)
0	49.20%
1	41.70%
2	37.20% †
3	32.70%
4	29.63% †
5	26.57% †
6	23.50%
7	22.42% †
8	21.35% †
9	20.27% †
10	19.20%
Note: † indicates linearly interpolated value.	

ULTRASONIC METHOD FOR INSPECTION OF THE STAYBOLTS

The inspection method for ultrasonic examination of the Reactor Process Water System heat exchanger staybolts is based on a pulse-echo straight beam technique. This technique allows the in-situ, in-service inspection of the staybolts from the outside of the staybolt housing, through the welded concave sealing cap and water gap to one end of a staybolt. Figure 8 illustrates the typical staybolt enclosure assembly.

The behavior of the ultrasonic beam propagating through boundaries of very dissimilar medium (couplant layer, sealing cap, water gap and the machined countersinks at the centers of both ends of the staybolts) resulted in multiple reflections. All factors and limitations associated with the examination including reflection at the interfaces, high attenuation, noise, scattering, beam spread, near and far fields, mode conversion, wavelength, frequency and velocity, geometric configuration, non-applicability of S-wave due to a water gap, were taken into consideration in the development of the UT technique. A transducer fixture mounted to the staybolt housing was designed, resulting in a successful technique for the inspection with flaw sizing capability greater than 25% of the staybolt diameter. Figure 9, provided for basic information only on how the technique works, shows the ultrasonic beam trace from the point where a high frequency mechanical vibration is leaving the generating element of the transducer until a reflected signal from the opposite end of the staybolt, and/or from a defect inside of the staybolt, is displayed on the CRT screen. This technique has been validated in mock-ups and is capable of collecting necessary test data for determination of the staybolt integrity and detecting planar flaws.

ACKNOWLEDGMENT

The information contained in this article was developed during the course of work done under Contract No. DE-AC09-89SR18035 with the U.S. Department of Energy.

REFERENCES

1) Aerospace Structural Metals Handbook, Volume 2, "Non-Ferrous Alloys", Code 1302, Figure 3.0313 "Tensile Properties of Annealed Bar at Room and Elevated Temperatures - Types 303 or 303 Se", March 1972.

2) ASM Metals Handbook, Volume 1 Tenth Edition, "Properties and Selection: Irons, Steels and High Performance Alloys", 1990.

3) Stoner, K.J., Sindelar, R.L. and Caskey, G.R., "Reactor Materials Program - Baseline Material Property Handbook - Mechanical Properties of 1950's Vintage Stainless Steel Weldment Components (U)," WSRC-TR-91-10, Westinghouse Savannah River Co., Aiken, SC, April 1,1991.

4) ASME Boiler and Pressure Vessel Code, Section III - Division 1 Appendices, 1988 Addenda .

5) Ranganath, S. and Mehta, H.S., "Engineering Methods for the Assessment of Ductile Fracture Margin in Nuclear Power Plant Piping," in Elastic-Plastic Fracture: Second Symposium, Volume II, ASTM STP 803, C.F. Shih and J.P. Gudas, Eds., American Society for Testing and Materials, 1983, pp. II-309 to 330.

6) PATRAN Plus, Release 2.5, PDA Engineering, Costa Mesa, California, October 1990.

7) ABAQUS, Version 4-8, Hibbitt, Karlsson & Sorensen, Inc., Pawtucket, Rhode Island, 1989.

8) Dynamic Seismic Analysis of Process Piping Systems, Savannah River Plant, Volume 1 Technical Approach and Summary of Results (Revision 1), URS/JAB 7233, URS/John Blume & Associates, Engineers, San Francisco, California, May 1983.

9) Tada, H., Paris, P.C., and Irwin, G.R., The stress Analysis of Cracks Handbook, 2nd. Edi., Paris Productions Inc. (and Del Research Corp.), Saint Louis, MO, 1985, page 2.10.

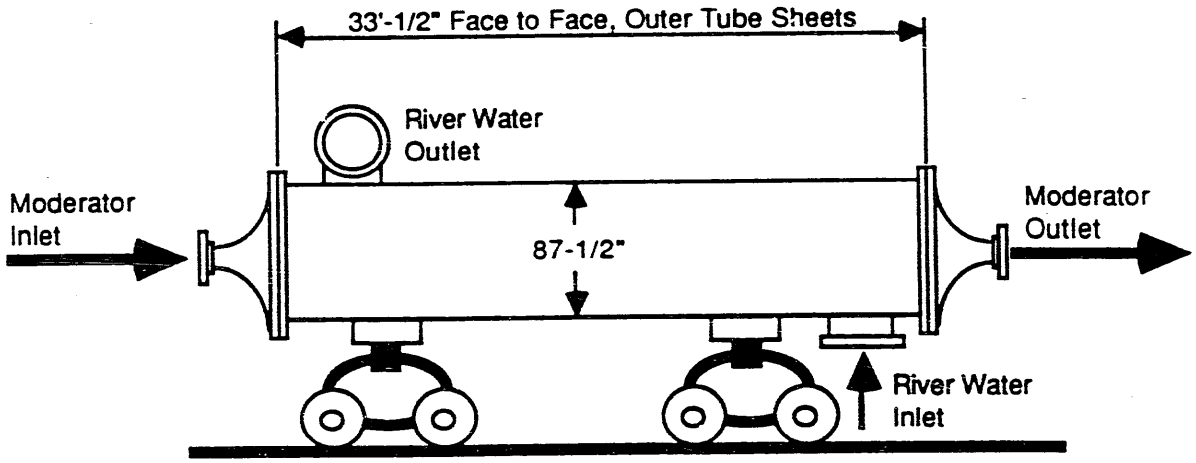

Figure 1 General View of SRS Heat Exchanger

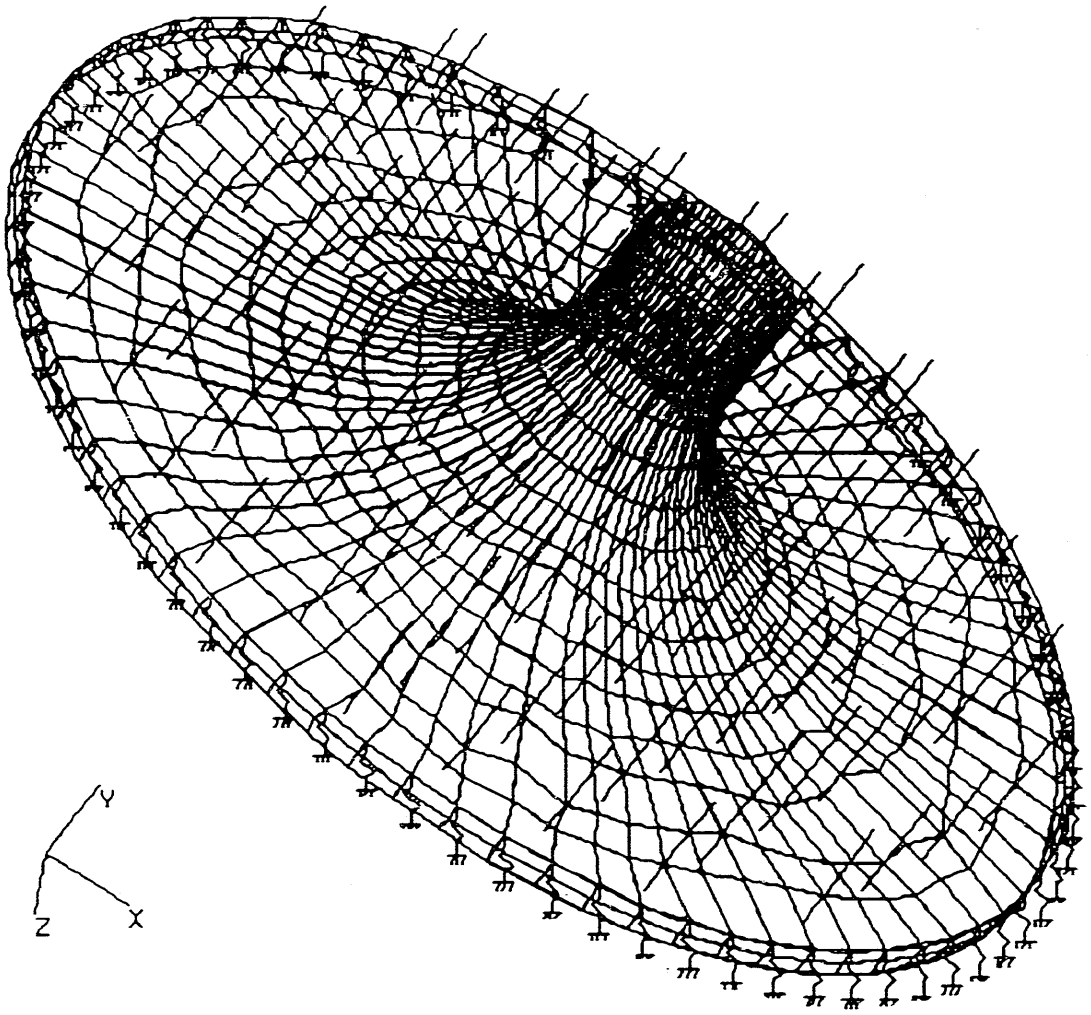

Figure 2 Finite Element Mesh for SRS Heat Exchanger Head

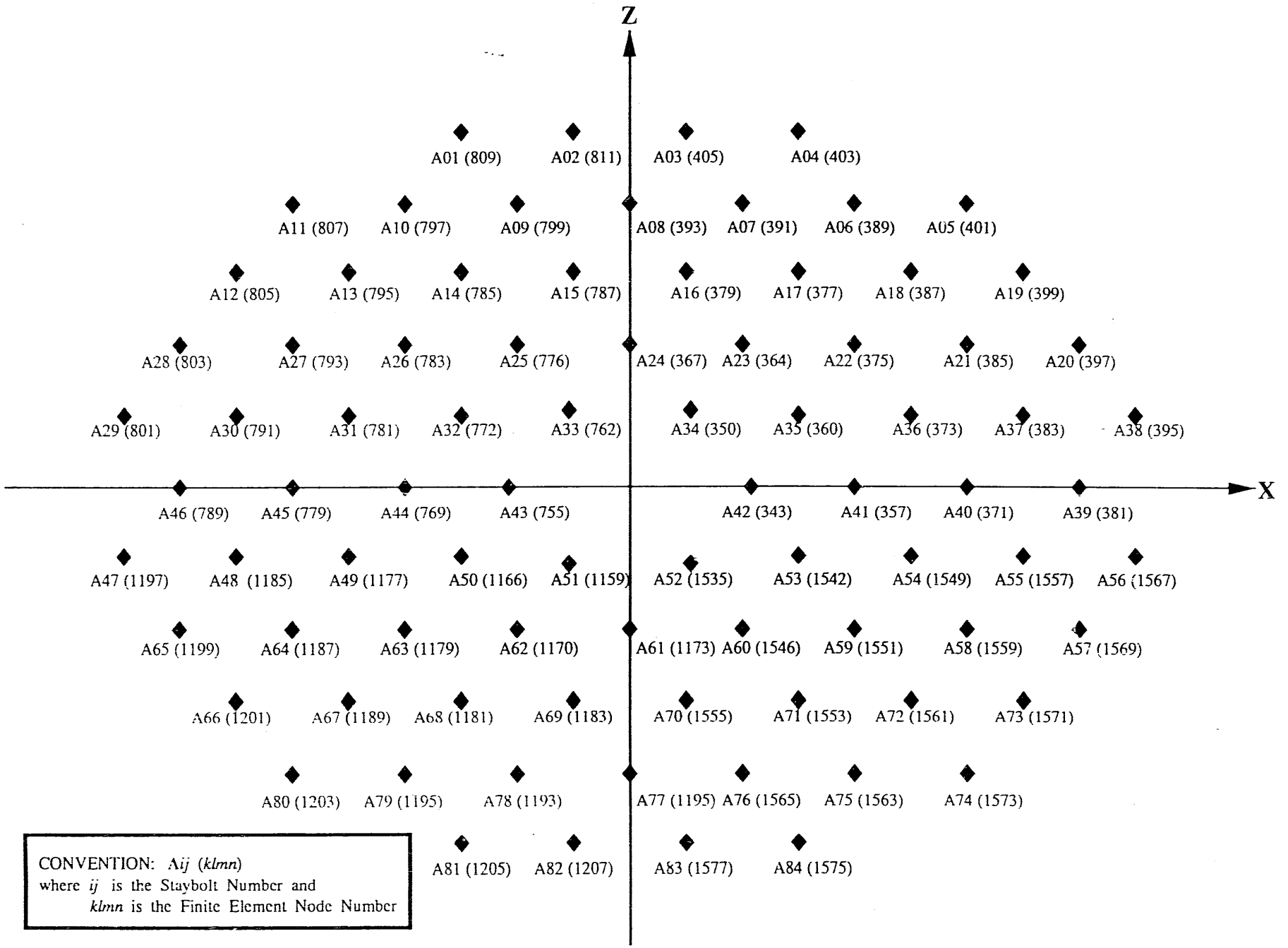

Figure 3 Staybolt Identification Numbers (Finite Element Node Numbers)

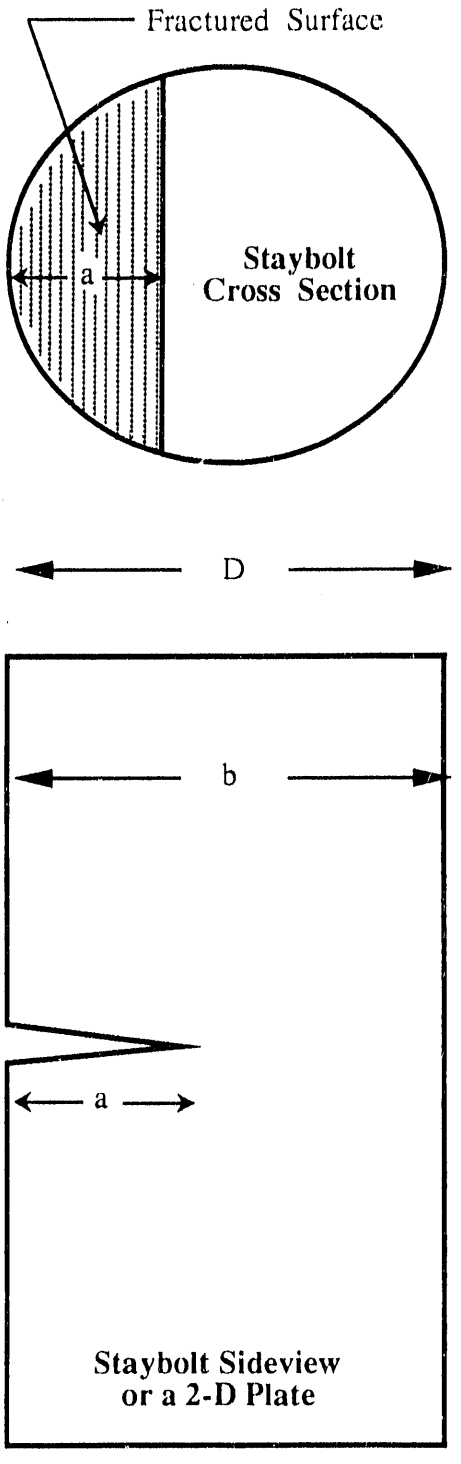

Figure 4 Fracture Analysis: Flawed Staybolt

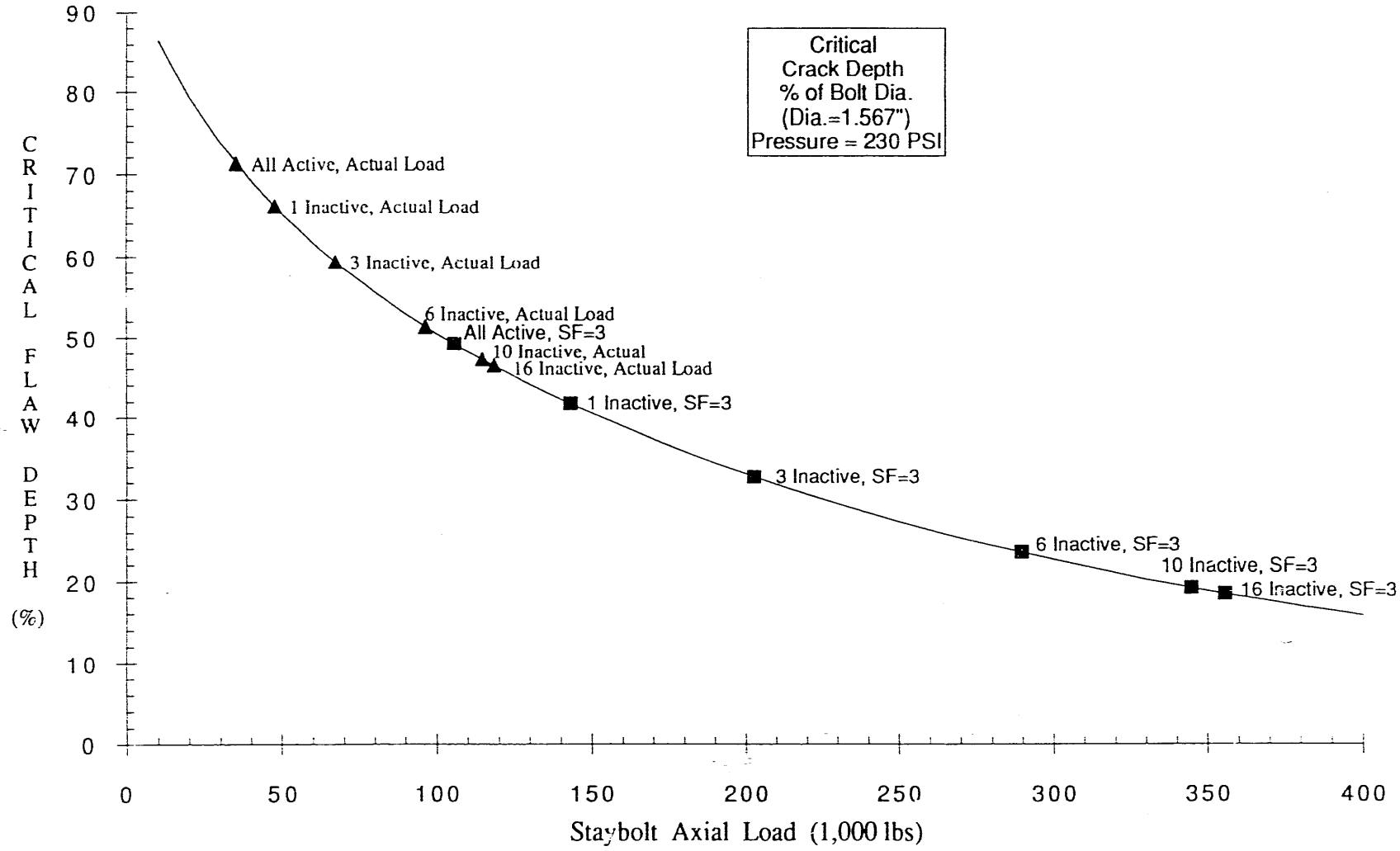

Figure 5 Instability Flaw Depth vs. Staybolt Axial Load

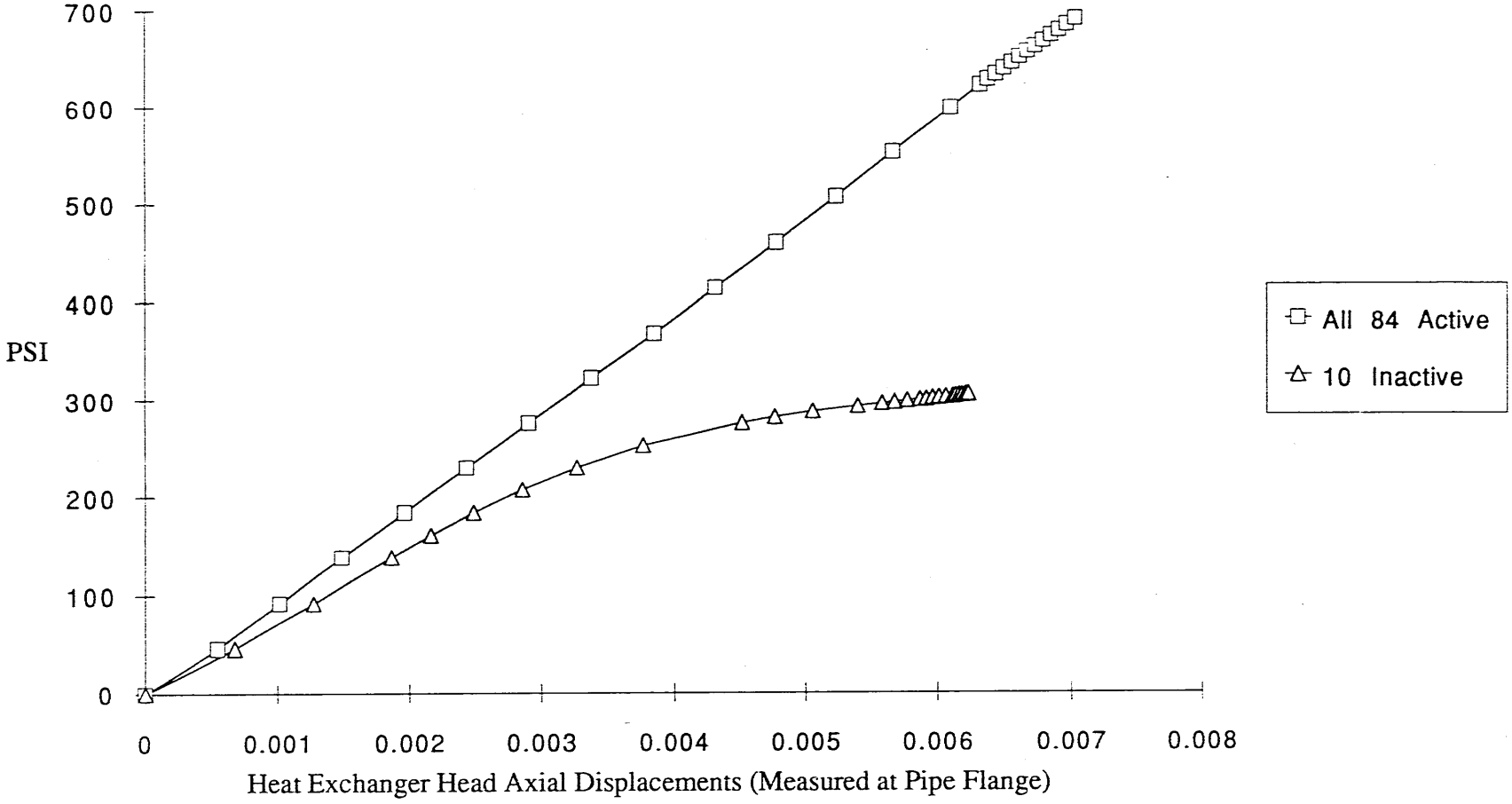

Figure 6 Heat Exchanger Head Load-Deflection Curves for Intact Head and 10 Inactive-Staybolt Configuration (Collapse Load Analyses)

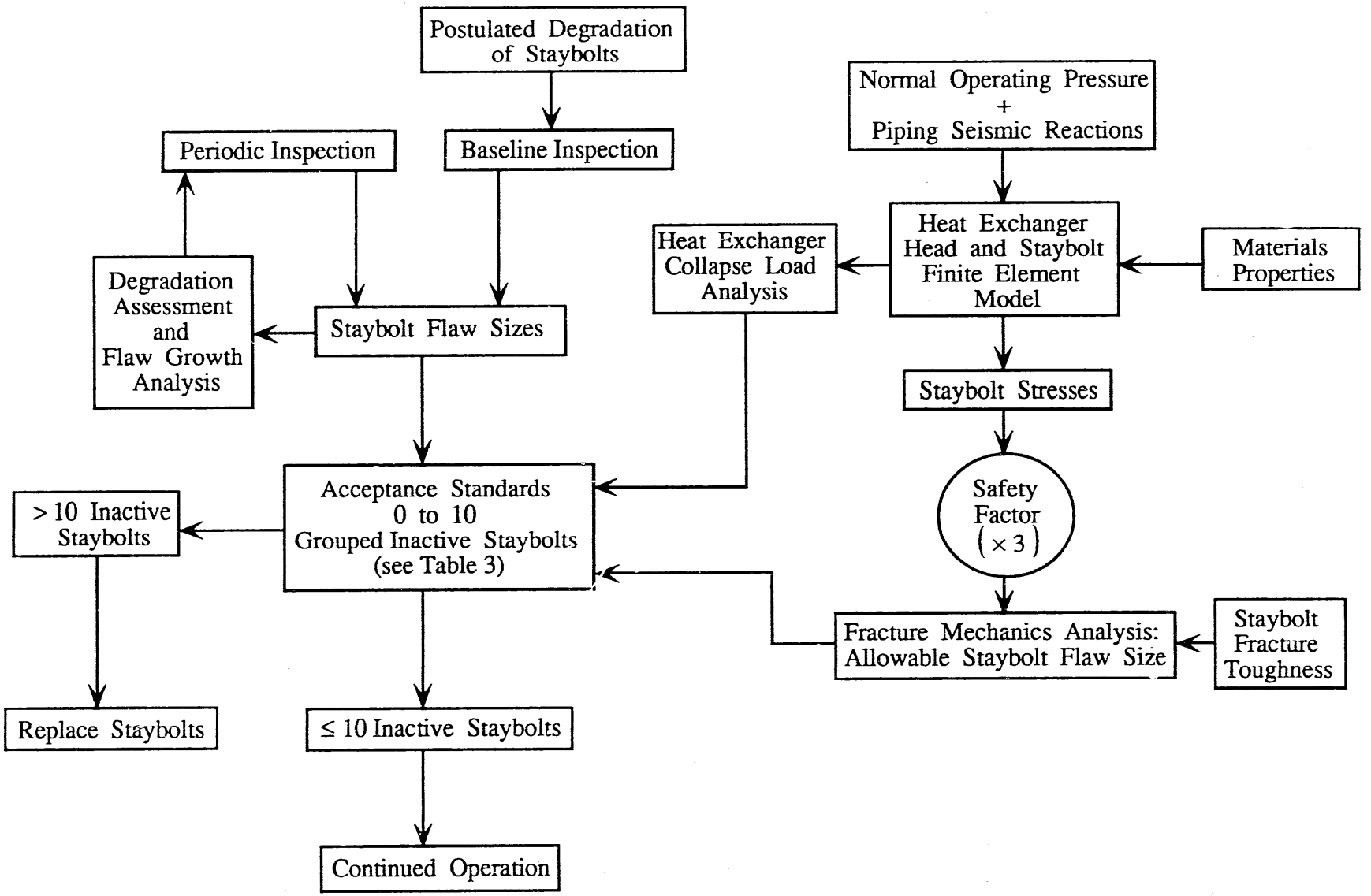

Figure 7 Heat Exchanger Staybolt Acceptance Criteria Methodology

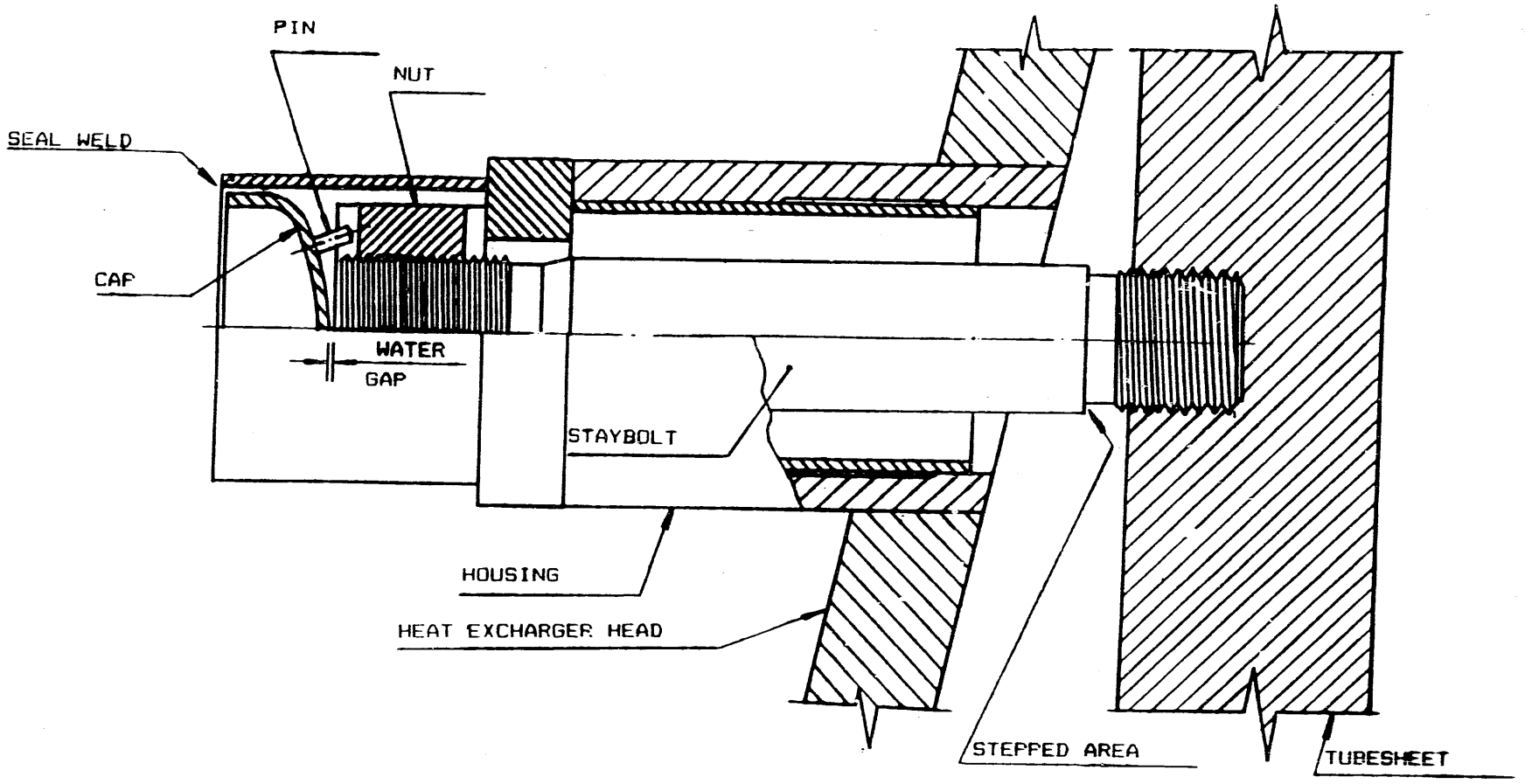

Figure 8 Staybolt Enclosure Assembly

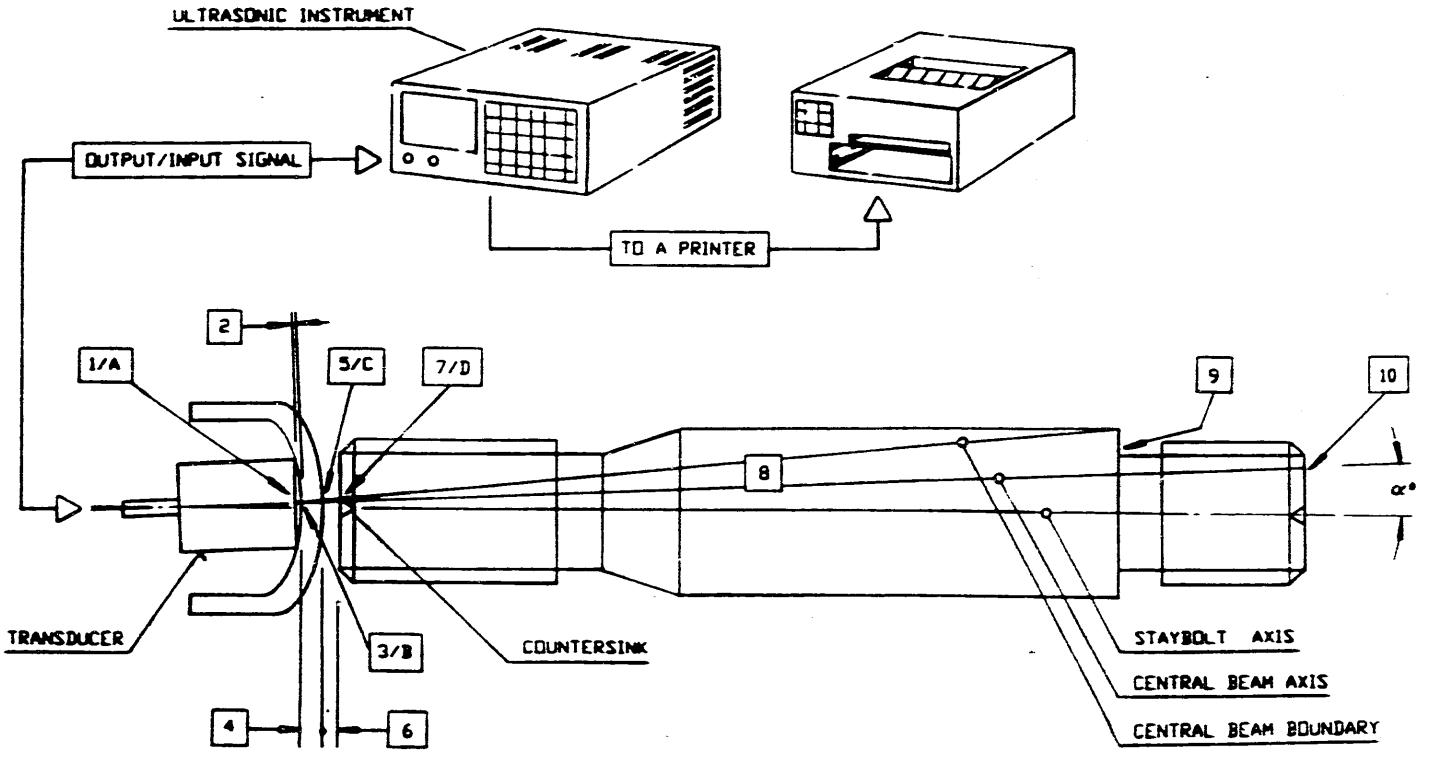

SOUND BEAM PATH:

1. Interface A, Element Protection Layer / Couplant
2. Couplant
3. Interface B, Couplant / Cap Entry Surface
4. Cap, Stainless Steel
5. Interface C, Cap Inner Surface / Water
6. Water
7. Interface D, Water / Staybolt Entry Surface
8. Staybolt, Fine Grain Stainless Steel
9. Staybolt Stepped Area
10. Staybolt Back Surface / Water

Figure 9 In Situ UT Inspection of Heat Exchanger Staybolts

END

DATE FILMED

5/22/92